

Measurement of Open Beauty Production at HERA

H1 Collaboration

Abstract

The first observation of open b production in ep collisions is reported. An event sample containing muons and jets has been selected which is enriched in semileptonic b quark decays. The visible cross section $\sigma(ep \rightarrow b\bar{b}X \rightarrow \mu X')$ for $Q^2 < 1 \text{ GeV}^2$, $0.1 < y < 0.8$ is measured to be $0.176 \pm 0.016 \text{ (stat.) } {}^{+0.026}_{-0.017} \text{ (syst.) nb}$ for the muons to be detected in the range $35^\circ < \theta^\mu < 130^\circ$ and $p_\perp^\mu > 2.0 \text{ GeV}$ in the laboratory frame. The expected visible cross section based on a NLO QCD calculation is $0.104 \pm 0.017 \text{ nb}$. The cross sections for electroproduction with $Q^2 < 1 \text{ GeV}^2$ and photoproduction are derived from the data and found to be $\sigma(ep \rightarrow e b\bar{b}X) = 7.1 \pm 0.6 \text{ (stat.) } {}^{+1.5}_{-1.3} \text{ (syst.) nb}$ and $\sigma(\gamma p \rightarrow b\bar{b}X) = 111 \pm 10 \text{ (stat.) } {}^{+23}_{-20} \text{ (syst.) nb}$ at an average $\langle W_{\gamma p} \rangle \sim 180 \text{ GeV}$, respectively.

Submitted to Physics Letters B

C. Adloff³³, V. Andreev²⁴, B. Andrieu²⁷, V. Arkadov³⁴, A. Astvatsatourov³⁴, I. Ayyaz²⁸, A. Babaev²³,
 J. Bähr³⁴, P. Baranov²⁴, E. Barrelet²⁸, W. Bartel¹⁰, U. Bassler²⁸, P. Bate²¹, A. Beglarian^{10,39},
 O. Behnke¹⁰, C. Beier¹⁴, A. Belousov²⁴, T. Benisch¹⁰, Ch. Berger¹, G. Bernardi²⁸, T. Berndt¹⁴,
 G. Bertrand-Coremans⁴, P. Biddulph²¹, J.C. Bizot²⁶, V. Boudry²⁷, W. Braunschweig¹, V. Brisson²⁶,
 H.-B. Bröker², D.P. Brown²¹, W. Brückner¹², P. Bruel²⁷, D. Bruncko¹⁶, J. Bürger¹⁰, F.W. Büsser¹¹,
 A. Bunyatyan^{12,39}, S. Burke¹⁷, A. Burrage¹⁸, G. Buschhorn²⁵, D. Calvet²², A.J. Campbell¹⁰,
 J. Cao²⁶, T. Carli²⁵, E. Chabert²², M. Charlet⁴, D. Clarke⁵, B. Clerbaux⁴, C. Collard⁴, J.G. Contreras^{7,41},
 J.A. Coughlan⁵, M.-C. Cousinou²², B.E. Cox²¹, G. Cozzika⁹, J. Cvach²⁹, J.B. Dainton¹⁸, W.D. Dau¹⁵,
 K. Daum^{33,38}, M. David^{9,†}, M. Davidsson²⁰, B. Delcourt²⁶, R. Demirchyan^{10,39}, A. De Roeck¹⁰,
 E.A. De Wolf⁴, C. Diaconu²², P. Dixon¹⁹, V. Dodonov¹², K.T. Donovan¹⁹, J.D. Dowell³, A. Droutskoi²³,
 C. Duprel², J. Ebert³³, G. Eckerlin¹⁰, D. Eckstein³⁴, V. Efremenko²³, S. Egli³⁶, R. Eichler³⁵,
 F. Eisele¹³, E. Eisenhandler¹⁹, E. Elsen¹⁰, M. Erdmann^{10,40,f}, A.B. Fahr¹¹, P.J.W. Faulkner³,
 L. Favart⁴, A. Fedotov²³, R. Felst¹⁰, J. Feltesse⁹, J. Ferencei¹⁰, F. Ferrarotto³¹, S. Ferron²⁷,
 M. Fleischer¹⁰, G. Flügge², A. Fomenko²⁴, I. Foresti³⁶, J. Formánek³⁰, J.M. Foster²¹, G. Franke¹⁰,
 E. Gabathuler¹⁸, K. Gabathuler³², J. Garvey³, J. Gassner³², J. Gayler¹⁰, R. Gerhards¹⁰, S. Ghazaryan^{10,39},
 A. Glazov³⁴, L. Goerlich⁶, N. Gogitidze²⁴, M. Goldberg²⁸, I. Gorelov²³, C. Grab³⁵, H. Grässler²,
 T. Greenshaw¹⁸, R.K. Griffiths¹⁹, G. Grindhammer²⁵, T. Hadig¹, D. Haidt¹⁰, L. Hajduk⁶, V. Hausteijn³³,
 W.J. Haynes⁵, B. Heinemann¹⁰, G. Heinzelmann¹¹, R.C.W. Henderson¹⁷, S. Hengstmann³⁶,
 H. Henschel³⁴, R. Heremans⁴, G. Herrera^{7,41,l}, I. Herynek²⁹, M. Hilgers³⁵, K.H. Hiller³⁴, C.D. Hilton²¹,
 J. Hladký²⁹, P. Höting², D. Hoffmann¹⁰, R. Horisberger³², S. Hurling¹⁰, M. Ibbotson²¹, Ç. İşsever⁷,
 M. Jacquet²⁶, M. Jaffre²⁶, L. Janauscek²⁵, D.M. Jansen¹², X. Janssen⁴, L. Jönsson²⁰, D.P. Johnson⁴,
 A. Zhokin²³, M. Jones¹⁸, H. Jung²⁰, H.K. Kästli³⁵, D. Kant¹⁹, M. Kapichine⁸, M. Karlsson²⁰,
 O. Karschnick¹¹, O. Kaufmann¹³, M. Kausch¹⁰, F. Keil¹⁴, N. Keller¹³, I.R. Kenyon³, S. Kermiche²²,
 C. Kiesling²⁵, M. Klein³⁴, C. Kleinwort¹⁰, G. Knies¹⁰, H. Kolanoski³⁷, S.D. Kolya²¹, V. Korbel¹⁰,
 P. Kostka³⁴, S.K. Kotelnikov²⁴, M.W. Krasny²⁸, H. Krehbiel¹⁰, J. Kroseberg³⁶, D. Krücker³⁷,
 K. Krüger¹⁰, A. Küpper³³, T. Kuhr¹¹, T. Kurča³⁴, W. Lachnit¹⁰, R. Lahmann¹⁰, D. Lamb³,
 M.P.J. Landon¹⁹, W. Lange³⁴, U. Langenegger³⁵, A. Lebedev²⁴, F. Lehner¹⁰, V. Lemaitre¹⁰,
 R. Lemrani¹⁰, V. Lendermann⁷, S. Levonian¹⁰, M. Lindstroem²⁰, V. Lubimov²³, G. Lobo²⁶,
 E. Lobodzinska¹⁰, S. Lüders³⁵, D. Lüke^{7,10}, L. Lytkin¹², N. Magnussen³³, H. Mahlke-Krüger¹⁰,
 N. Malden²¹, E. Malinovski²⁴, I. Malinovski²⁴, R. Maraček²⁵, P. Marage⁴, J. Marks¹³, R. Marshall²¹,
 H.-U. Martyn¹, J. Martyniak⁶, S.J. Maxfield¹⁸, T.R. McMahon¹⁸, A. Mehta⁵, K. Meier¹⁴, P. Merkel¹⁰,
 F. Metlica¹², A. Meyer¹⁰, H. Meyer³³, J. Meyer¹⁰, P.-O. Meyer², S. Mikocki⁶, D. Milstead¹⁸,
 R. Mohr²⁵, S. Mohrdieck¹¹, M.N. Mondragon⁷, F. Moreau²⁷, A. Morozov⁸, J.V. Morris⁵, D. Müller³⁶,
 K. Müller¹³, P. Murín^{16,42}, V. Nagovizin²³, B. Naroska¹¹, J. Naumann⁷, Th. Naumann³⁴, I. Négri²²,
 P.R. Newman³, H.K. Nguyen²⁸, T.C. Nicholls⁵, F. Niebergall¹¹, C. Niebuhr¹⁰, O. Nix¹⁴, G. Nowak⁶,
 T. Nunnemann¹², J.E. Olsson¹⁰, A. Usik²⁴, D. Ozerov²³, P. Palmen², V. Panassik⁸, C. Pascaud²⁶,
 S. Passaggio³⁵, G.D. Patel¹⁸, H. Pawletta², E. Perez⁹, J.P. Phillips¹⁸, D. Pitzl³⁵, R. Pöschl⁷,
 I. Potashnikova¹², B. Povh¹², K. Rabbertz¹, G. Rädcl⁹, J. Rauschenberger¹¹, P. Reimer²⁹, B. Reisert²⁵,
 D. Reyna¹⁰, S. Riess¹¹, E. Rizvi³, P. Robmann³⁶, R. Roosen⁴, A. Rostovtsev^{23,10}, C. Royon⁹,
 S. Rusakov²⁴, K. Rybicki⁶, D.P.C. Sankey⁵, J. Scheins¹, F.-P. Schilling¹³, S. Schleif¹⁴, P. Schleper¹³,
 D. Schmidt³³, D. Schmidt¹⁰, L. Schoeffel⁹, T. Schörner²⁵, V. Schröder¹⁰, H.-C. Schultz-Coulon¹⁰,
 F. Sefkow³⁶, V. Shekelyan²⁵, I. Sheviakov²⁴, L.N. Shtarkov²⁴, G. Siegmon¹⁵, Y. Sirois²⁷, T. Sloan¹⁷,
 P. Smirnov²⁴, M. Smith¹⁸, V. Solochenko²³, Y. Soloviev²⁴, V. Spaskov⁸, A. Specka²⁷, H. Spitzer¹¹,
 R. Stamen⁷, J. Steinhart¹¹, B. Stella³¹, A. Stellberger¹⁴, J. Stiewe¹⁴, U. Straumann¹³, W. Struczinski²,
 J.P. Sutton³, M. Swart¹⁴, M. Taševský²⁹, V. Tchernyshov²³, S. Tchetchelnitski²³, G. Thompson¹⁹,
 P.D. Thompson³, N. Tobien¹⁰, R. Todenhausen¹², D. Traynor¹⁹, P. Truöl³⁶, G. Tsipolitis³⁵,
 J. Turnau⁶, J. Turney¹⁹, E. Tzamariudaki²⁵, S. Udluft²⁵, S. Valkár³⁰, A. Valkárová³⁰, C. Vallée²²,
 A. Van Haecke⁹, P. Van Mechelen⁴, Y. Vazdik²⁴, G. Villet⁹, S. von Dombrowski³⁶, K. Wacker⁷,
 R. Wallny¹³, T. Walter³⁶, B. Waugh²¹, G. Weber¹¹, M. Weber¹⁴, D. Wegener⁷, A. Wegner¹¹,

T. Wengler¹³, M. Werner¹³, L.R. West³, G. White¹⁷, S. Wiesand³³, T. Wilksen¹⁰, M. Winde³⁴, G.-G. Winter¹⁰, Ch. Wissing⁷, M. Wobisch², H. Wollatz¹⁰, E. Wunsch¹⁰, J. Žáček³⁰, J. Zálešák³⁰, Z. Zhang²⁶, P. Zini²⁸, F. Zomer²⁶, J. Zsembery⁹ and M. zur Nedden¹⁰

¹ I. Physikalisches Institut der RWTH, Aachen, Germany^a

² III. Physikalisches Institut der RWTH, Aachen, Germany^a

³ School of Physics and Space Research, University of Birmingham, Birmingham, UK^b

⁴ Inter-University Institute for High Energies ULB-VUB, Brussels; Universitaire Instelling Antwerpen, Wilrijk; Belgium^c

⁵ Rutherford Appleton Laboratory, Chilton, Didcot, UK^b

⁶ Institute for Nuclear Physics, Cracow, Poland^d

⁷ Institut für Physik, Universität Dortmund, Dortmund, Germany^a

⁸ Joint Institute for Nuclear Research, Dubna, Russia

⁹ DSM/DAPNIA, CEA/Saclay, Gif-sur-Yvette, France

¹⁰ DESY, Hamburg, Germany^a

¹¹ II. Institut für Experimentalphysik, Universität Hamburg, Hamburg, Germany^a

¹² Max-Planck-Institut für Kernphysik, Heidelberg, Germany^a

¹³ Physikalisches Institut, Universität Heidelberg, Heidelberg, Germany^a

¹⁴ Institut für Hochenergiephysik, Universität Heidelberg, Heidelberg, Germany^a

¹⁵ Institut für experimentelle und angewandte Physik, Universität Kiel, Kiel, Germany^a

¹⁶ Institute of Experimental Physics, Slovak Academy of Sciences, Košice, Slovak Republic^{f,j}

¹⁷ School of Physics and Chemistry, University of Lancaster, Lancaster, UK^b

¹⁸ Department of Physics, University of Liverpool, Liverpool, UK^b

¹⁹ Queen Mary and Westfield College, London, UK^b

²⁰ Physics Department, University of Lund, Lund, Sweden^g

²¹ Department of Physics and Astronomy, University of Manchester, Manchester, UK^b

²² CPPM, Université d'Aix-Marseille II, IN2P3-CNRS, Marseille, France

²³ Institute for Theoretical and Experimental Physics, Moscow, Russia

²⁴ Lebedev Physical Institute, Moscow, Russia^{f,k}

²⁵ Max-Planck-Institut für Physik, München, Germany^a

²⁶ LAL, Université de Paris-Sud, IN2P3-CNRS, Orsay, France

²⁷ LPNHE, École Polytechnique, IN2P3-CNRS, Palaiseau, France

²⁸ LPNHE, Universités Paris VI and VII, IN2P3-CNRS, Paris, France

²⁹ Institute of Physics, Academy of Sciences of the Czech Republic, Praha, Czech Republic^{f,h}

³⁰ Nuclear Center, Charles University, Praha, Czech Republic^{f,h}

³¹ INFN Roma 1 and Dipartimento di Fisica, Università Roma 3, Roma, Italy

³² Paul Scherrer Institut, Villigen, Switzerland

³³ Fachbereich Physik, Bergische Universität Gesamthochschule Wuppertal, Wuppertal, Germany^a

³⁴ DESY, Zeuthen, Germany^a

³⁵ Institut für Teilchenphysik, ETH, Zürich, Switzerlandⁱ

³⁶ Physik-Institut der Universität Zürich, Zürich, Switzerlandⁱ

³⁷ Present address: Institut für Physik, Humboldt-Universität, Berlin, Germany^a

³⁸ Also at Rechenzentrum, Bergische Universität Gesamthochschule Wuppertal, Wuppertal, Germany^a

³⁹ Visitor from Yerevan Physics Institute, Armenia

⁴⁰ Also at Institut für Experimentelle Kernphysik, Universität Karlsruhe, Karlsruhe, Germany

⁴¹ Also at Dept. Fis. Ap. CINVESTAV, Mérida, Yucatán, México

⁴² Also at University of P.J. Šafárik, SK-04154 Košice, Slovak Republic

[†] Deceased

^a Supported by the Bundesministerium für Bildung, Wissenschaft, Forschung und Technologie, FRG, under contract numbers 7AC17P, 7AC47P, 7DO55P, 7HH17I, 7HH27P, 7HD17P, 7HD27P, 7KI17I, 6MP17I and 7WT87P

^b Supported by the UK Particle Physics and Astronomy Research Council, and formerly by the UK Science and Engineering Research Council

^c Supported by FNRS-FWO, IISN-IIKW

^d Partially supported by the Polish State Committee for Scientific Research, grant no. 115/E-343/SPUB/P03/002/97 and grant no. 2P03B 055 13

^e Supported in part by US DOE grant DE F603 91ER40674

^f Supported by the Deutsche Forschungsgemeinschaft

^g Supported by the Swedish Natural Science Research Council

^h Supported by GA ČR grant no. 202/96/0214, GA AV ČR grant no. A1010821 and GA UK grant no. 177

ⁱ Supported by the Swiss National Science Foundation

^j Supported by VEGA SR grant no. 2/5167/98

^k Supported by Russian Foundation for Basic Research grant no. 96-02-00019

^l Supported by the Alexander von Humboldt Foundation

Introduction

The study of heavy quark production in electron–proton scattering provides an important testing ground for QCD. Measurements of open charm production [1] at the electron-proton collider, HERA, have been shown to be reasonably well described by next to leading order (NLO) QCD calculations [2, 3, 4, 5] based on the photon-gluon fusion mechanism. It is essential to extend these observations and tests of QCD to the production of heavier quarks.

In the past, the leptonproduction of open b quarks has been too difficult to observe due to the small production cross section. At fixed target experiments only upper limits on the leptonproduction cross section have been published [6, 7, 8]¹. In this paper, the first observation of b quark leptonproduction is presented in the range Q^2 less than 1 GeV², where Q^2 is the four-momentum transfered from the electron to the proton. This corresponds to the exchange of an almost real photon (photoproduction) i.e. $Q^2 \sim 0$.

The data were collected at the HERA collider with the H1 detector during 1996 and correspond to an integrated luminosity of $\mathcal{L} = 6.6 \text{ pb}^{-1}$. The production of b quarks is observed through their semileptonic decay to muons. The production cross section is measured in a kinematic range determined by the properties of the muon from the heavy quark decay and is compared with the prediction of a NLO QCD calculation for partons [3] to which a model for the hadronisation and semileptonic decays is added.

Detector Description

Only a short description of the detector components which play a major role in this analysis is given here; a detailed description of the detector and its trigger capabilities can be found elsewhere [9]. Charged particles are measured by two cylindrical jet drift chambers (CJC) [10], mounted concentrically around the beam line inside a homogeneous magnetic field of 1.15 Tesla, yielding measurements of particle momenta in the polar angular range² of 20° to 160°. Two double layers of cylindrical multiwire proportional chambers [11] with pad read-out for triggering purposes are positioned inside and in between the two drift chambers. The tracking detector is surrounded by a fine grained liquid argon calorimeter [12], covering a polar angle range of 4° to 154°, consisting of an electromagnetic section with lead absorbers and a hadronic section with steel absorbers. Muons are measured as tracks in the CJC and identified by demanding a good link to a track in the instrumented iron return yoke which surrounds the superconducting coil. For events from deep–inelastic scattering (DIS) at higher Q^2 the scattered electron is detected by a “spaghetti–type” lead-scintillator-fibre calorimeter (Spacal) [13] which covers the backward region of the detector up to a polar angle of 177.8°.

Analysis Procedure

The production of b quarks is detected by looking for muons from the semileptonic decay of a b hadron inside jets from the hadronisation of the b quark. A sample of events enriched in semileptonic decays of b quarks is selected by demanding that each event has at least 2 jets and

¹EMC also derived a cross section based on the observation of one clear event [6].

²H1 uses a right-handed coordinate system with the z -axis pointing in the direction of the proton beam (forward) and the x -axis pointing towards the centre of the storage ring.

that at least one of the jets should contain a muon. The jets are built by using both the calorimetric and track information and are identified by using a cone algorithm [14] with a cone radius $r = \sqrt{(\Delta\eta)^2 + (\Delta\phi)^2} < 1$, where ϕ is the azimuthal angle and η is the pseudorapidity and with transverse energy to the beam direction, E_T , of more than 6 GeV. The muon is required to be in the central region of the detector ($35^\circ < \theta^\mu < 130^\circ$) and to have a transverse momentum with respect to the beam direction, p_\perp^μ , of more than 2 GeV. The selected events have a mean track multiplicity of 16.5 and a minimum of at least 5 tracks per event is required. The events are triggered by requiring the existence of a muon candidate in coincidence with tracks. The trigger efficiency to select these events is determined directly from the data to be $85.5 \pm 1.6\%$ and is found to be constant for $p_\perp^\mu > 2$ GeV. To suppress contributions from DIS at higher Q^2 the events which contained an electron candidate with more than 4 GeV energy deposited in the Spacal are rejected. To avoid regions of high radiative corrections and to eliminate the remaining DIS events, the value of y was limited to the range $0.1 < y < 0.8$. Here y is $q \cdot P / \ell \cdot P$ where q , P and ℓ are the four momenta of the virtual photon, incident proton and lepton, respectively. It is calculated using the Jacquet-Blondel method [15]. These conditions limit the data sample to photoproduction events with $Q^2 < 1 \text{ GeV}^2$; the mean Q^2 is $6 \cdot 10^{-2} \text{ GeV}^2$. In total 927 events fulfil these selection criteria.

Beauty is separated from charm and other backgrounds on a statistical basis using the transverse momentum of the muon, $p_{T,rel}^\mu$, measured relative to the thrust axis of the jet which contains it. The thrust axis is defined as the direction such that

$$T = \max \frac{\sum |p_i^L|}{\sum |p_i|},$$

where the sums run over all the neutral and charged particles in the jet with the exception of the muon. Here, p_i is the momentum and p_i^L its longitudinal component with respect to the thrust axis. Since the b quark is heavy, it is expected that the $p_{T,rel}^\mu$ spectrum is harder for events originating from b quark decays than for decays from lighter quarks. For the determination of the beauty cross section, the $p_{T,rel}^\mu$ spectrum is used for a combined fit of the different contributions to the selected data sample. The shapes of the b and c contributions to the $p_{T,rel}^\mu$ are taken from the AROMA Monte Carlo [16] event generator, which is based on leading order (LO) QCD matrix elements, with the photon directly interacting with the partons in the proton and additional initial and final state parton showers.

The method relies on a good understanding of the energy flow within jets, for jets originating from heavy quarks, and on a correct determination of the muon misidentification probability. To check that the Monte Carlo simulation describes the energy distribution within jets, a data sample enriched in charm quarks is studied, where events with at least one jet and at least one D^* candidate are selected. The $D^{*\pm}$ candidate is identified through the decay $D^{*+} \rightarrow D^0 \pi^+ \rightarrow K^- \pi^+ \pi^+$ and its charge conjugate. This gives a sample of events with 20% background which has been verified to have a similar distribution to charm. In each of these events jets are identified using the same selection criteria as in the muon sample. The energy flow within the jet has been compared to the energy flow as given by the AROMA Monte Carlo event generator for charm events with a D^* . There is a good agreement between the data and the prediction from the Monte Carlo (see figure 1). From this and many other such comparisons it is concluded that the Monte Carlo simulation reliably models the data distributions.

The selected sample contains muons originating from the semileptonic decays of b and c quarks as well as from light hadrons which are misidentified as muons, due to decay or hadronic energy leakage (punchthrough). To obtain the background contribution originating

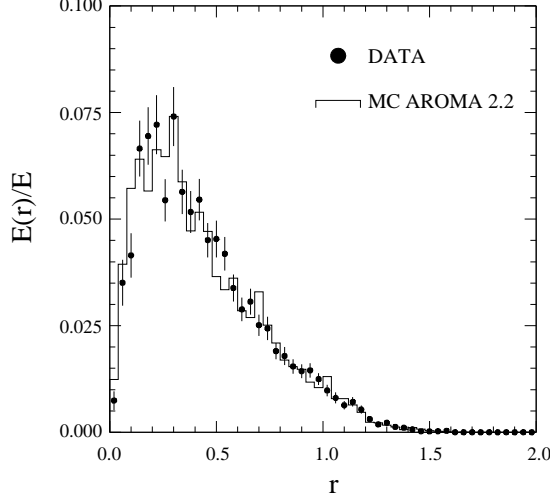


Figure 1: Fractional energy flow within jets as a function of the distance to the jet axis. This fraction is the ratio of the energy in an annulus at radius r to the total energy in the jet. The data points (filled dots) correspond to a data sample of mainly charm decays and the full histogram to a Monte Carlo simulation where only charm quarks are generated. Both the data and Monte Carlo are normalized so that the integral of the distributions equals one.

from misidentifying a light hadron as a muon, it is essential to know the probability $\mathcal{P}_h^\mu(p, \theta)$ for this to occur. Large samples of single pion, kaon and proton tracks are passed through the full detector simulation and the fraction measured as muons is determined. From these, the misidentification probability functions $\mathcal{P}_h^\mu(p, \theta)$, where $h = \pi, K, p$, are parameterised as a function of the momentum and the polar angle of the hadron. These functions vary with the polar angle but do not exceed $6 \cdot 10^{-3}$ in the case of pions and $2 \cdot 10^{-2}$ in the case of kaons. For protons it is found to be below $2 \cdot 10^{-3}$. These probability functions are verified in the data by studying K_S^0 and ϕ decays, as a source of real pions and kaons, respectively. The distributions of fake muons agree both in shape and absolute magnitude (figure 2) with those predicted by applying the probability functions to the pions from K_S^0 decays. For kaons from ϕ decays, 8 fake muons are observed compared to 7.8 predicted. These observations show that the probability functions are well determined.

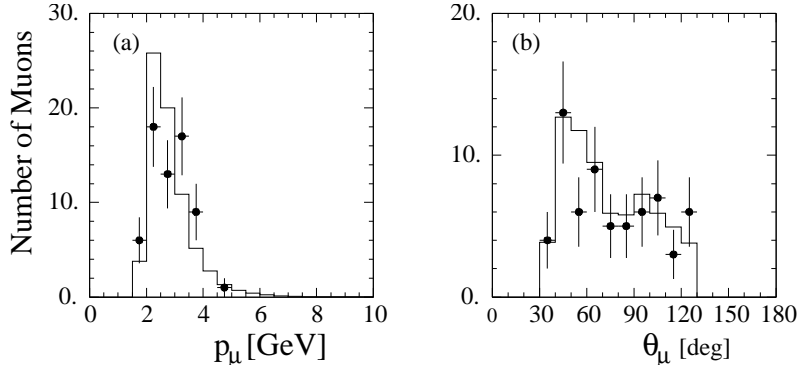


Figure 2: Momentum (a) and polar angle (b) distributions for fake muons in a pion sample from the decay $K_S^0 \rightarrow \pi^+ \pi^-$. The filled points show the fake muon yield as measured in the data. The solid histogram gives the estimate of the muon yield as obtained by assigning $\mathcal{P}_h^\mu(p, \theta)$ as a weight to every pion and summing the weights over the entire pion sample. The measured yield is 64 fake muons; the estimate amounts to 69.8.

The knowledge of the $\mathcal{P}_h^\mu(p, \theta)$ functions allows the background from hadrons, which are falsely identified as muons in the $p_{T,rel}^\mu$ spectrum, to be calculated in shape and absolute magnitude from the data. For this purpose, events with at least two jets with $E_T > 6$ GeV each, but without the muon requirement, are selected. The expected background in the $p_{T,rel}^\mu$ distribution is calculated from all hadrons which pass the p_\perp^μ and polar angle requirements. The assignment of a hadron as a pion, kaon or proton is made using the JETSET[17] specification of the fractions of these particles which is in agreement with measurements by the SLD and DELPHI collaborations [18]. The JETSET pion and kaon fractions are varied by ± 0.05 , covering the largest deviation of JETSET from these measurements. This variation corresponds to about 15% relative variation of the kaon fraction. The result of this variation is included in the systematic error for this background determination.

Results

The observed $p_{T,rel}^\mu$ distribution is shown in figure 3 together with the b signal and the different

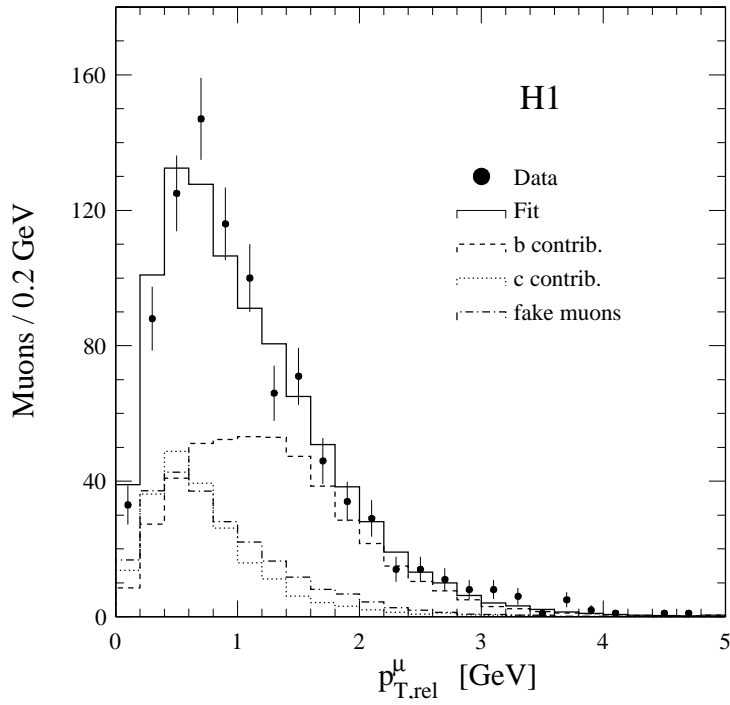


Figure 3: The measured $p_{T,rel}^\mu$ distribution in the data and the fitted sum (solid line) of the contributions of beauty (dashed line), charm (dotted line) and the fixed fake muon background (dashed-dotted line).

background contributions. The signal and backgrounds are obtained from the combined fit of the b and c contributions, using the shapes from the AROMA Monte Carlo, together with the fake muon background determined as described above. The relative composition of the data sample amounts to $f_b = 50.8 \pm 4.9\%$ (beauty), $f_c = 22.4 \pm 5.0\%$ (charm), and $f_{fake} = 25.9\%$ (background, fixed). The uncertainty of the latter is included in the systematic error which is deduced by changing the pion and kaon fractions as described above.

The visible electroproduction cross section for b quarks, determined from the number of muon events attributed to b quark decays, is measured to be:

$$\sigma_{vis}(ep \rightarrow b\bar{b}X \rightarrow \mu X') = 0.176 \pm 0.016 (stat.) {}^{+0.026}_{-0.017} (syst.) \text{ nb}$$

in the kinematic range $Q^2 < 1 \text{ GeV}^2$, $0.1 < y < 0.8$, $p_{\perp}^{\mu} > 2.0 \text{ GeV}$ and $35^\circ < \theta^{\mu} < 130^\circ$, where the first uncertainty is statistical and the second systematic.

The acceptance is determined from the AROMA Monte Carlo simulation to be 24%, of which the efficiency for muon identification is 56% and the probability to reconstruct two jets each with $E_T > 6 \text{ GeV}$ is 42.9%. The full analysis has been repeated using the HERWIG 5.9 [19] and RAPGAP [20] Monte Carlo simulations assuming both direct and resolved production of the c and b quarks. In addition, different E_T cuts for the jets and different values of the Peterson fragmentation parameter, ε , for both the c and b fragmentation have been used. The variation of the cross section with the different simulations amounts to $\pm 7.1\%$ and this is taken to be the systematic error due to the uncertainties in the Monte Carlo. The systematic uncertainty due to the muon reconstruction is $+6\%$. The systematic error due to the uncertainty ($\pm 4\%$) in the hadronic energy scale of the calorimeter is $\pm 4.9\%$. The systematic uncertainty from the luminosity calculation is $\pm 1.8\%$. The error due to the background shape and magnitude is found to be $^{+9.5}_{-3.6}\%$ by changing the assumption on the π, K, p composition in the measured hadron sample, as described above, as well as by using event samples selected by different triggers of the experiment to estimate the background.

To estimate the theoretically expected cross section, the NLO QCD calculation by Frixione *et al.* (FMNR) [3] is used, with $m_b = 4.75 \text{ GeV}$ and the MRSB [21] and GRV-HO [22] structure functions for the proton and photon, respectively. This program supplies the kinematics of the b quarks. In order to determine the expectation for the kinematic range where the measurement is performed, the b quarks are fragmented to mesons and then allowed to decay semileptonically. For the b quark fragmentation the Peterson parameterisation [23] is used with $\varepsilon_b = 0.006 \pm 0.003$ [24]. If the fragmentation is done by simply scaling the b quark four vector by the factor generated according to the Peterson function the expected cross section in the visible range is $\sigma(ep \rightarrow b\bar{b}X \rightarrow \mu X') = 0.118 \text{ nb}$. However, if the hadronisation of the b quark is done together with the generation of a light quark pair then the expected cross section in the visible range is $\sigma(ep \rightarrow b\bar{b}X \rightarrow \mu X') = 0.089 \text{ nb}$. This difference is due to a softer transverse momentum distribution of the b hadron in the latter case, which influences the p_{\perp}^{μ} spectrum where a cut is applied. For the theoretical expectation the average of the above values is taken and the difference is taken to be the systematic uncertainty. A variation in the renormalisation or factorisation scale, which is defined as $\mu_R = \mu_F = \sqrt{m_b^2 + p_{\perp,b}^2}$, by a factor of 2 changes the expected cross section by $\pm 10\%$. This uncertainty is added in quadrature to the uncertainty due to the fragmentation. The theoretically expected cross section based on a NLO QCD calculation is therefore taken to be $0.104 \pm 0.017 \text{ nb}$ to be compared to the measured value of $0.176 \pm 0.016 \text{ (stat.) } ^{+0.026}_{-0.017} \text{ (syst.) nb}$. The expectation from the FMNR calculation in LO for $\sigma(ep \rightarrow b\bar{b}X \rightarrow \mu X')$ is $0.069 \pm 0.008 \text{ nb}$. The corresponding LO QCD expectation from the AROMA generator, with which this measurement has been compared previously [25], is 0.038 nb .

In the Weizsäcker-Williams approximation (WWA)[26] the electroproduction cross section, σ_{ep} , is expressed as a convolution of the flux of photons emitted by the electron, $f_{e/\gamma}$, with the photoproduction cross section :

$$\sigma_{ep} = \sigma(ep \rightarrow e b\bar{b}X) = \int dy f_{e/\gamma} \sigma(\gamma p \rightarrow b\bar{b}X).$$

In order to derive the total photoproduction cross section the measured σ_{ep} in the visible kinematic range has to be extrapolated to the full phase space. The fraction of the phase space

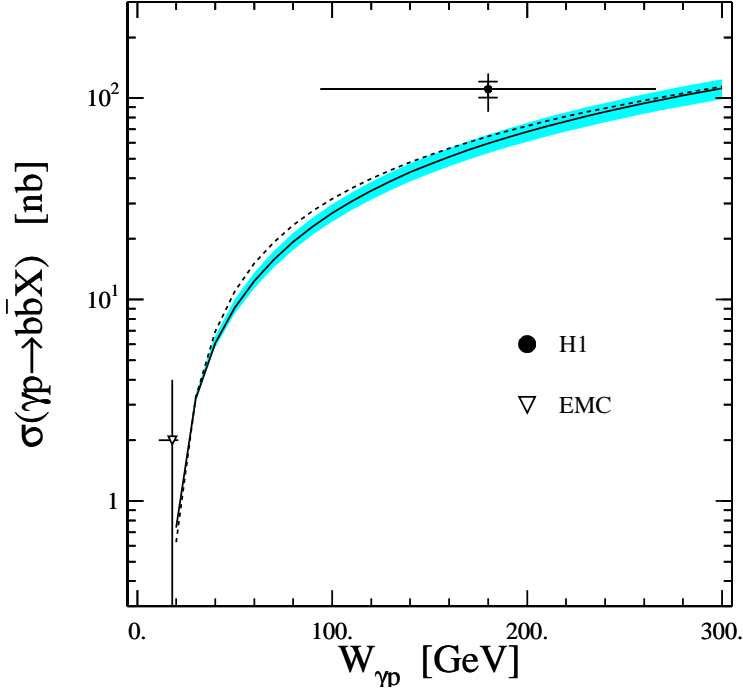


Figure 4: The total photoproduction cross section, $\sigma(\gamma p \rightarrow b \bar{b} X)$. The horizontal error bar represents the range of the measurement. The solid curve shows the expectation of the FMNR NLO QCD calculation (full line) with $m_b = 4.75$ GeV and the MRS/GRV-HO structure functions for the proton and the photon, respectively. The shaded area corresponds to the uncertainty if the factorisation scale changes by a factor of 2. A change of the renormalisation scale by a factor of 2 leads to a similar result. The dashed line represents the prediction of the FMNR NLO QCD calculation if the MRST [28] structure function for the proton is used.

covered by the defined visible range is found to be 12.5%, from the FMNR NLO calculation with the hadronization and semileptonic decay, as described above. Correcting for the semileptonic branching fractions for a muon originating from a b quark [27] and extrapolating to the full phase space, the total electroproduction cross section for $Q^2 < 1 \text{ GeV}^2$ is $\sigma(ep \rightarrow e b \bar{b} X) = 7.1 \pm 0.6^{+1.0}_{-0.7} \pm 1.1$ nb. Using the WWA the total photoproduction cross section is $\sigma(\gamma p \rightarrow b \bar{b} X) = 111 \pm 10^{+16}_{-11} \pm 17$ nb averaged over the range $94 < W_{\gamma p} < 266$ GeV with a mean value of $\langle W_{\gamma p} \rangle \sim 180$ GeV. Here the first and second errors are the experimental statistical and systematic uncertainties, respectively. The third is the systematic error due to the extrapolation and the branching fraction uncertainties for the semileptonic b quark decays [27]. The expectation of the FMNR NLO calculation is 63 nb. This measurement together with that from EMC and the expectation of the FMNR NLO QCD calculation are shown in figure 4.

Conclusion

The open b production cross section has been measured for the first time at HERA using semi-muonic decays of the b quarks. The visible cross section $\sigma(ep \rightarrow b \bar{b} X \rightarrow \mu X')$, in the range $Q^2 < 1 \text{ GeV}^2$, $0.1 < y < 0.8$, $p_{\perp}^{\mu} > 2.0$ GeV and $35^\circ < \theta^{\mu} < 130^\circ$, is found to be 0.176 ± 0.016 (stat.) $^{+0.026}_{-0.017}$ (syst.) nb, compared to the expectation 0.104 ± 0.017 nb from a NLO QCD calculation.

From this measurement the total cross section for electroproduction with $Q^2 < 1 \text{ GeV}^2$ and photoproduction, extrapolated to the full phase space, is calculated to be $\sigma(ep \rightarrow e b \bar{b} X) = 7.1 \pm 0.6(\text{stat.})_{-1.3}^{+1.5}(\text{syst.}) \text{ nb}$ and $\sigma(\gamma p \rightarrow b \bar{b} X) = 111 \pm 10(\text{stat.})_{-20}^{+23}(\text{syst.}) \text{ nb}$ at an average $\langle W_{\gamma p} \rangle \sim 180 \text{ GeV}$, respectively. The measured cross sections are higher than the expectation based on a NLO QCD calculation.

Acknowledgements

We are grateful to the HERA machine group whose outstanding efforts have made and continue to make this experiment possible. We thank the engineers and technicians for their work in constructing and now maintaining the H1 detector, the funding agencies for financial support, the DESY technical staff for continual assistance, and the DESY directorate for the hospitality extended to the non-DESY members of the collaboration. We would like to thank S. Frixione for enlightening discussions on the NLO QCD calculation program.

References

- [1] H1 Collab., C. Adloff *et al.*, *Z. Phys. C* **72**, 593 (1996);
ZEUS Collab., J. Breitweg *et al.*, *Phys. Lett. B* **407**, 402 (1997);
H1 Collab., C. Adloff *et al.*, *Nucl. Phys. B* **545**, 21 (1999);
ZEUS Collab., J. Breitweg *et al.*, *DESY 99-101*, Submitted to *E. Phys. J. C*.
- [2] R.K. Ellis, and P. Nason, *Nucl. Phys. B* **312**, 551 (1989).
- [3] S. Frixione, M.L. Mangano, P. Nason and G. Ridolfi, *Phys. Lett. B* **348**, 633 (1995).
- [4] J. Smith and W. L. van Neerven, *Nucl. Phys. B* **374**, 36 (1992).
- [5] B.W. Harris and J. Smith, *Nucl. Phys. B* **452**, 109 (1995); *Phys. Lett. B* **412**, 535 (1995).
- [6] EMC, J.-J. Aubert *et al.*, *Phys. Lett. B* **106**, 419 (1981).
- [7] BCDMS Collab., A.C. Benvenuti *et al.*, *Phys. Lett. B* **158**, 531 (1985).
- [8] BFP Collab., W.H. Smith *et al.*, *Phys. Rev. D* **25**, 2762 (1982).
- [9] H1 Collab., I. Abt *et al.*, *Nucl. Instrum. Methods A* **386**, 310 (1997).
- [10] J. Bürger *et al.*, *Nucl. Instrum. Methods A* **279**, 217 (1989).
- [11] K. Müller *et al.*, *Nucl. Instrum. Methods A* **312**, 457 (1992).
- [12] B. Andrieu *et al.*, *Nucl. Instrum. Methods A* **336**, 460 (1993).
- [13] R.-D. Appuhn *et al.*, *Nucl. Instrum. Methods A* **386**, 397 (1997).
- [14] M.H. Seymour, *Z. Phys. C* **62**, 127 (1994).
- [15] F. Jacquet and A. Blondel, *Proceedings of the Study of an ep facility for Europe*, Ed. U. Amaldi, DESY 79/48, 391.

- [16] G. Ingelman, J. Rathsmann and G. A. Schuler, *Comp. Phys. Com.* **101**, 135 (1997).
- [17] T. Sjöstrand and M. Bengtsson, *Comp. Phys. Com.* **43**, 367 (1987).
- [18] DELPHI Collab., P. Abreu *et al.*, *E. Phys. J. C* **5**, 585 (1998);
SLD Collab., K. Abe *et al.*, *Phys. Rev. D* **59**, 052001 (1999).
- [19] G. Marchesini *et al.*, *Comp. Phys. Com.* **67**, 465 (1992).
- [20] H. Jung, *Comp. Phys. Com.* **86**, 147 (1995);
(for update see <http://www-h1.desy.de/~jung/rapgap/rapgap.html>).
- [21] A.D. Martin, R.G. Roberts and W.J. Stirling, *Phys. Lett. B* **354**, 155 (1995).
- [22] M. Glück, E. Reya and A. Vogt, *Phys. Rev. D* **45**, 3986 (1992); *Phys. Rev. D* **46**, 1973 (1992).
- [23] C. Peterson *et al.*, *Phys. Rev. D* **27**, 105 (1983).
- [24] P. Nason and C. Oleari, *Phys. Lett. B* **447**, 327 (1999).
- [25] H1 Collab., Conf. Paper 575, 29th Intern. Conf. on High-Energy Physics, Vancouver, Canada (1998)
- [26] C.F. Weizsäcker, *Z.Phys* **88**, 612 (1934);
E.J. Williams, *Phys.Rev.* **45**, 729 (1934).
- [27] Particle Data Group, C. Caso *et al.*, *E. Phys. J. C* **3**, 1 (1998).
- [28] A.D. Martin, R.G. Roberts, W.J. Stirling and R.S. Thorne, *E. Phys. J. C* **4**, 463 (1998).